Solar forcing of winter climate variability in the Northern Hemisphere

Sarah Ineson[1]*, Adam A. Scaife[1], Jeff R. Knight[1], James C. Manners[1], Nick J. Dunstone[1], Lesley J. Gray[2] and Joanna D. Haigh[3]

An influence of solar irradiance variations on Earth's surface climate has been repeatedly suggested, based on correlations between solar variability and meteorological variables[1]. Specifically, weaker westerly winds have been observed in winters with a less active sun, for example at the minimum phase of the 11-year sunspot cycle[2-4]. With some possible exceptions[5,6], it has proved difficult for climate models to consistently reproduce this signal[7,8]. Spectral Irradiance Monitor satellite measurements indicate that variations in solar ultraviolet irradiance may be larger than previously thought[9]. Here we drive an ocean–atmosphere climate model with ultraviolet irradiance variations based on these observations. We find that the model responds to the solar minimum with patterns in surface pressure and temperature that resemble the negative phase of the North Atlantic or Arctic Oscillation, of similar magnitude to observations. In our model, the anomalies descend through the depth of the extratropical winter atmosphere. If the updated measurements of solar ultraviolet irradiance are correct, low solar activity, as observed during recent years, drives cold winters in northern Europe and the United States, and mild winters over southern Europe and Canada, with little direct change in globally averaged temperature. Given the quasiregularity of the 11-year solar cycle, our findings may help improve decadal climate predictions for highly populated extratropical regions.

Satellite observations of solar spectral irradiance in the ultraviolet region have been subject to uncertainty; the Solar Stellar Irradiance Comparison Experiment and Spectral Irradiance Monitor (SIM) instruments aboard the Solar Radiation and Climate Experiment (SORCE) satellite mission (2004–present) are the first designed to achieve accurate long-term measurements of the solar irradiance variations over the entire ultraviolet range[9]. The 200–320 nm part of the ultraviolet band contributes strongly to solar heating in the middle atmosphere, largely through ozone absorption. Ozone is itself produced through the interaction between ultraviolet radiation and oxygen, giving rise to potential positive feedback[10]. SORCE observations made during the decline of solar cycle 23 reveal a remarkably strong decrease in mid-ultraviolet flux, some four to six times greater[11] than previous spectral irradiance reconstructions[12]. However, before the SORCE mission, variations at these wavelengths were poorly constrained, with measurement uncertainty exceeding the potential solar-cycle variation[13]. Currently there are limited data (less than one solar cycle) so questions remain concerning accuracy and also applicability of the SIM data to other solar cycles[11,14].

We use the SIM observations of solar variability to estimate the change in ultraviolet radiation between the maximum and minimum of the 11-year solar cycle and impose this forcing on an ocean–troposphere–stratosphere–mesosphere climate model[15]. Our simulations are for 80 years of solar minimum and 80 years of solar maximum conditions. This experiment is designed to demonstrate the response in surface climate to the change in ultraviolet flux alone with a perturbation applied to the 200–320 nm model spectral band, and the solar irradiance flux at other wavelengths held constant. For simplicity we use monthly climatological ozone and ignore stratospheric ozone feedback[10] but note that this feedback would probably enhance the effects shown below.

In winter (December to February) the simulated and observed response at the solar minimum shows substantial changes over the whole northern hemisphere (Fig. 1). Model sea-level pressure increases at high northern latitudes and decreases at mid-latitudes in both the Pacific and Atlantic basins corresponding to a negative Arctic Oscillation or North Atlantic Oscillation-like pattern (AO/NAO; Fig. 1a). The observed response (Fig. 1b) also shows similarities in both structure and magnitude with the negative phase of the AO/NAO, although there is observational uncertainty in the Atlantic basin depending on the period analysed[16,17]. Quantifying the change in the AO sea-level pressure difference between mid-latitudes and the Arctic gives a shift of -1.2 hPa for the model, which is in good agreement with -1.1 hPa for the reanalysis. For the Atlantic sector alone, the change in the NAO is -2.4 hPa for the model, compared with an observed change of -4.6 hPa (Fig. 2a). Note the comparatively large uncertainty in the reanalysis data due to the small number of years relative to the model simulations, so that smaller, country-scale anomalies can differ. Also note the symmetry in the high- and low-solar-activity reanalysis response when compared with all years in the time series, suggesting at least a degree of linearity.

Consistent with the model surface pressure pattern, decreased westerly flow in the Atlantic sector leads to anomalously cold near-surface temperatures (Fig. 1c) over northeastern Europe and northern Asia and mild conditions further south. This is in reasonable agreement with observations (Fig. 1d) which also show negative anomalies extending over much of northern Eurasia. The regional difference in temperature between the solar maximum and solar minimum for northern Europe has sign and amplitude consistent with that in observations (Fig. 2b). Corresponding to the modelled decrease in the AO, we also see warming over northeastern North America and cooling over southeastern North America (Fig. 1c); however, no statistically significant changes (90% confidence level) are seen in the reanalysis in these regions (Fig. 1d).

The observed response to decreasing solar ultraviolet irradiance begins in the upper stratosphere and lower mesosphere, where
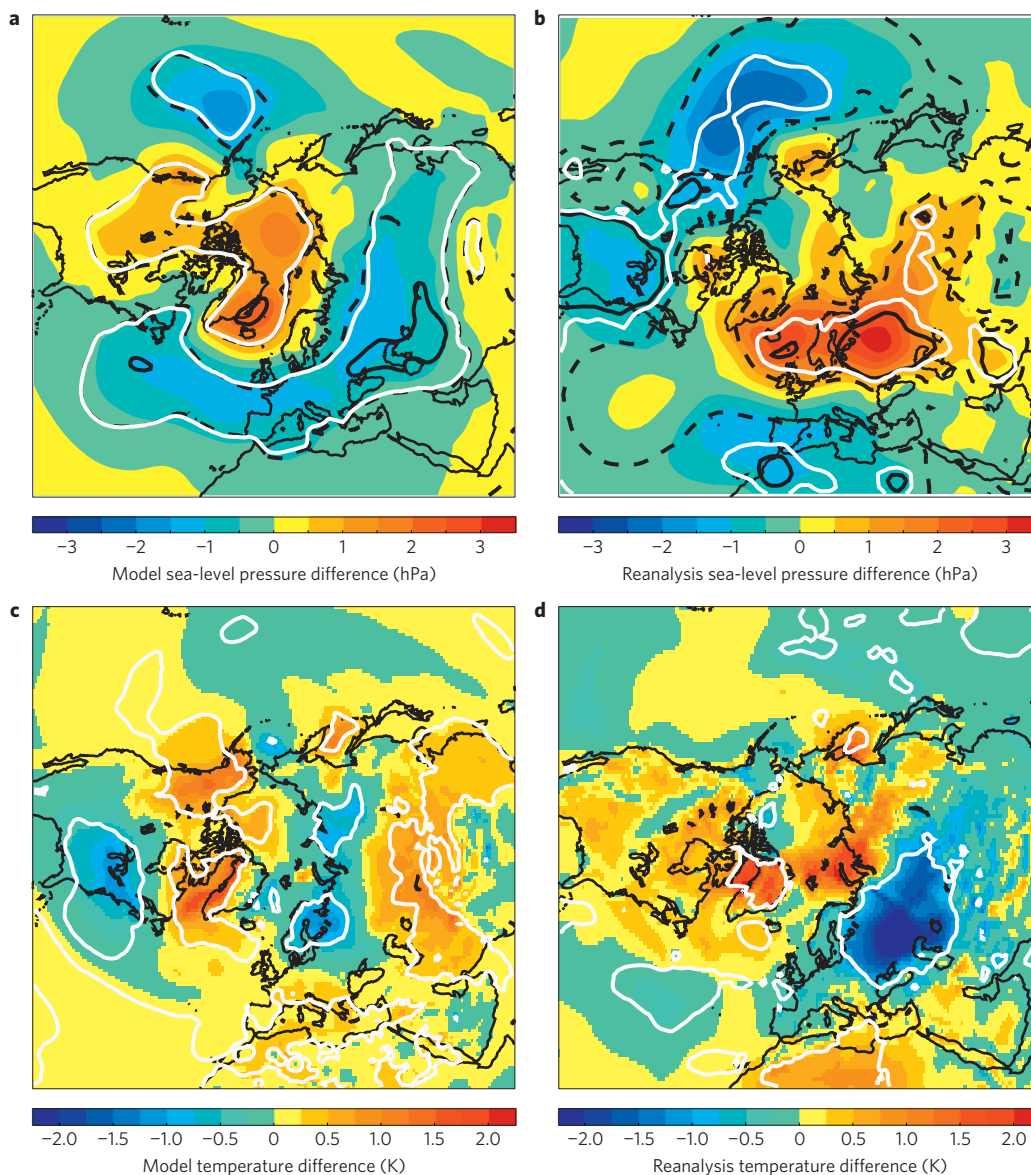

Figure 1 | Difference in winter surface climate for solar minimum minus solar maximum. a,b, Sea-level pressure difference for model (**a**) and ERA-40/ERA-Interim reanalysis (**b**). **c,d**, Near-surface temperature difference for model (**c**) and reanalysis (**d**). The differences are for December to February mean fields. The dashed (solid) black contours show the sea-level pressure difference relative to the interannual standard deviation at 25% (50%). The solid white contours indicate significance at the 95% confidence level for the model (**a,c**) and 90% for reanalyses (**b,d**). All panels are centred around the North pole.

satellite observations and ERA-40 reanalysis show a decrease in temperature of 1–2 K from the solar maximum to solar minimum[1]. This temperature change is directly attributable to the decrease in ozone heating associated with ultraviolet irradiance, which is important at these levels[11]. This signal peaks in the tropics and corresponds to a relative decrease in the pole-to-equator temperature gradient. This response is reproduced in our model (Supplementary Fig. S1) with significant cooling of about 2 K near the tropical stratopause. Geostrophic balance requires that the diminished polewards temperature gradient is matched by a weak easterly wind anomaly in the subtropical zonal mean circulation in the upper stratosphere. This anomaly has been observed to propagate polewards and downwards during autumn and winter and to amplify as it does so, giving a mid-stratospheric easterly shift of 5–10 m s^{-1} and a weaker polar vortex in December–January at the solar minimum[3,4]. This mechanism is reproduced in our model. Weak subtropical easterly anomalies of 1–2 m s^{-1}

are seen in October; these move polewards and downwards from November to February with a maximum amplitude anomaly of 5–6 m s^{-1} in January (Fig. 3a). Similar amplitude anomalies propagate polewards and downwards in the reanalysis (Fig. 3b).

Propagation and amplification of the easterly wind anomaly is associated with altered planetary wave activity[4,18]. Eliassen–Palm (EP) flux divergence simulated at the solar minimum indicates a greater easterly forcing (that is an increase in wave driving) of the polar night jet in the shear region below the maximum zonal wind anomaly (Fig. 4). This leads to a local deceleration and downwards propagation of the easterly anomaly. Large-scale wave forcing is therefore driving the development of the response in our model, in agreement with observational analyses[4] and earlier modelling studies[6]. Following this winter signal, during February and March a westerly anomaly develops at high altitude and moves polewards and downwards, in both the reanalysis and model (albeit more weakly in the model). Stratospheric oscillations are known to
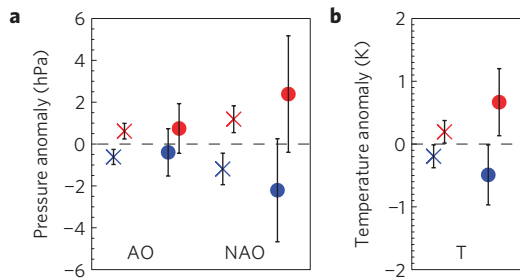
Figure 2 | Agreement between modelled and observed surface climate response. Winter (December to February) composite anomalies for solar minimum (blue) and solar maximum (red) for model (crosses) and reanalyses (circles). **a**, AO, sea-level pressure difference between mid-latitude (30°–55° N) and Arctic-latitude (65°–90° N) bands; NAO, sea-level pressure difference (hPa) between Azores and Iceland. **b**, T, near-surface temperature for Northern European region (0°–60° E, 50°–70° N). The vertical lines show the standard error.

occur even in the presence of steady tropospheric planetary wave forcing[19], and these late-winter westerly wind anomalies seem to be associated with a similar 'Polar Jet Oscillation'[4], with the initial easterly phase of the oscillation being determined by solar forcing as described above.

Signals in the lower stratosphere communicate a response throughout the depth of the troposphere, particularly in the storm-track regions (Fig. 1), and although the mechanism is still subject to debate it involves a dynamically balanced tropospheric response

to the stratospheric circulation change above, and occurs as a robust feature of experiments where the stratosphere is perturbed[20]. Altered development of baroclinic instability in the troposphere[21], or a feedback between the propagation of synoptic-scale eddies and the eddy-driven jet[22], may also be important.

Our experiment confirms a 'top-down', stratosphere-to-troposphere, pathway for the high-latitude response to recent observed solar variability with an altered westerly jet. The AO/NAO-like pattern and changes in atmospheric circulation that emerge from the model resemble the previous observed estimates of the effects of solar variability not only in pattern and evolution but also in amplitude through the autumn and winter seasons. Climate models, including those with comprehensive upper-atmosphere physics[7,8], have typically been inconsistent in simulating the observed extratropical response to the 11-year solar cycle, with the model response often weak or not significant. Our experiments suggest that underestimation of the ultraviolet component of the solar variability could provide a plausible explanation. This idea is supported by early experiments where larger but arbitrary imposed changes in ultraviolet flux in a numerical model reproduced the observed polewards and downwards evolution through internal dynamics[23]. The establishment of a large-enough upper-stratosphere meridional temperature gradient is crucial to this mechanism and we note that other recent studies show the model response in the equatorial upper stratosphere to be substantially larger with SIM data than with an earlier solar-variability reconstruction[11,24].

Other studies have discussed possible 'bottom-up' influences on surface climate through changes in surface radiative effects[25],
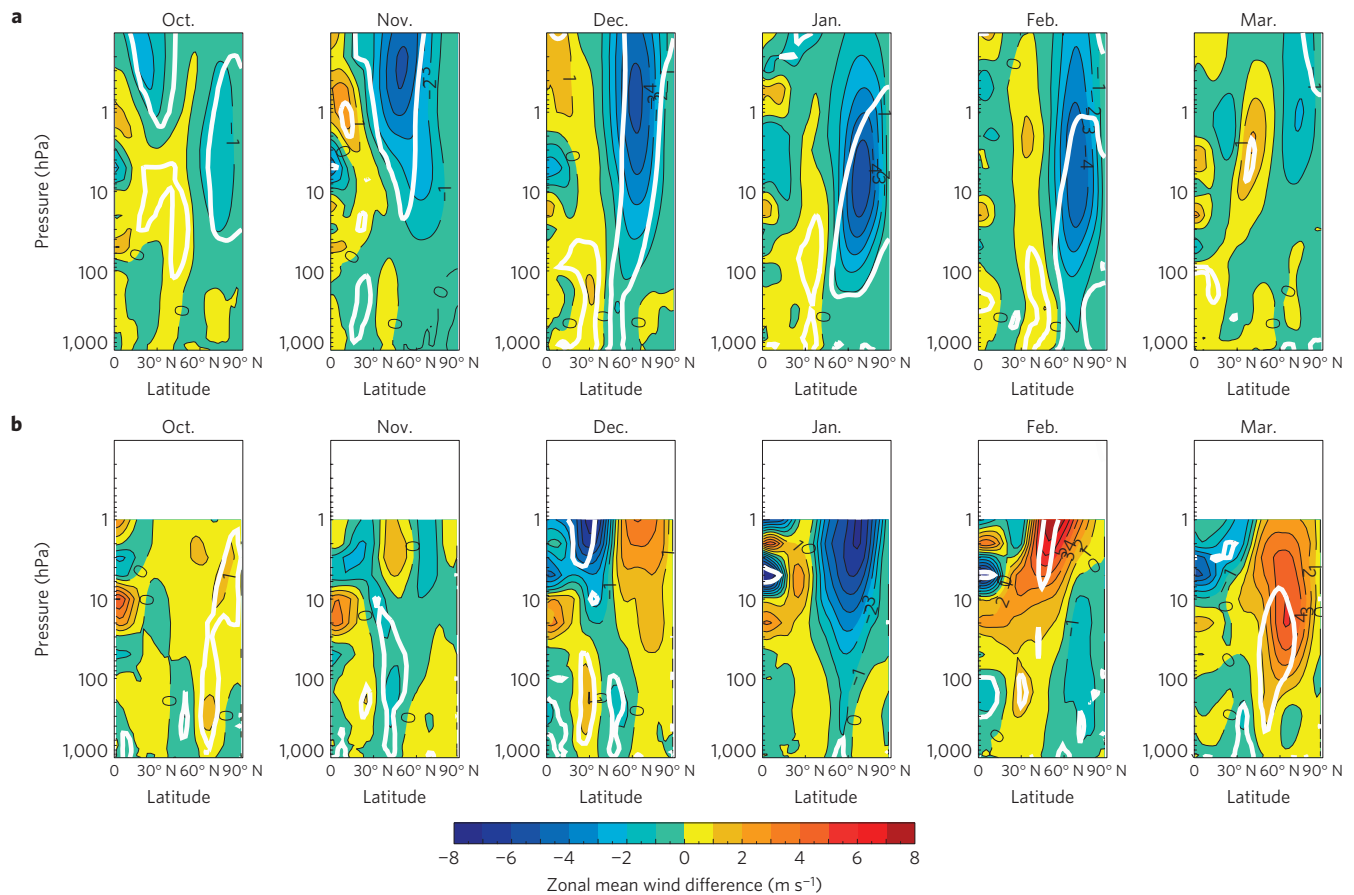

Figure 3 | Polewards and downwards progression of solar climate signal. a,b, Composite monthly zonal mean zonal wind (m s⁻¹) for the difference between the solar minimum and maximum for October to March in model (**a**) and reanalysis (**b**). The solid white contours indicate significance at the 95% confidence level for the model (**a**) and 90% for reanalysis (**b**).
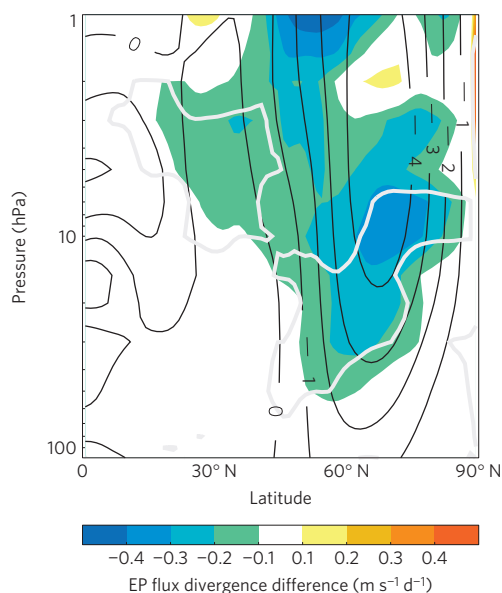
Figure 4 | Modelled large-scale wave driving of solar climate response.
Zonal mean zonal wind (m s^{-1}; contours) and EP flux divergence
(m s^{-1} d^{-1}; colours) for difference between solar minimum and maximum.
The differences are for January–February means. The EP flux divergence
has been scaled by the inverse of the pressure. The solid white contours
indicate significance at the 95% confidence level.

but we exclude this possibility from our runs as there are no
imposed changes to incoming radiation at visible wavelengths.
Our experiment demonstrates that the observed extratropical
circulation response can be driven from the new observational
estimates of ultraviolet variations alone. Likewise, our experiment
can say little about links between solar variability and global
mean temperature change[11,24]. We have also ignored possible
modulation by the quasibiennial oscillation (QBO) suggested in
some observational[2] and modelling[7] studies, although our model
does produce a spontaneous QBO.

The average of recent winters (2008/9, 2009/10 and 2010/11)
shows cold conditions over northern Europe and the United
States and mild conditions over Canada and the Mediterranean
associated with anomalously low and even record low values of
the NAO. This period also had easterly anomalies in the lower
stratosphere. Given our modelling result, these cold winters were
probably exacerbated by the recent prolonged and anomalously low
solar minimum[26]. On decadal timescales the increase in the NAO
from the 1960s to 1990s, itself known to be strongly connected to
changes in winter stratospheric circulation[20], may also be partly
explained by the upwards trend in solar activity evident in the open
solar-flux record[26]. There could also be confirmation of a leading
role for the 'top-down' influence of solar variability on surface
climate during periods of prolonged low solar activity such as the
Maunder minimum[27] if the ultraviolet variations used here also
apply to longer timescales.

The solar effect presented here contributes a substantial fraction
of typical year-to-year variations in near-surface circulation, with
shifts of up to 50% of the interannual variability (Fig. 1a,b).
This represents a substantial shift in the probability distribution
for regional winter climate and a potentially useful source of
predictability. Solar variability is therefore an important factor
in determining the likelihood of similar winters in future.
However, mid-latitude climate variability depends on many factors,
not least internal variability, and forecast models that simulate
all the relevant drivers are needed to estimate the range of
possible winter conditions.

Our result has important implications for regional climate
prediction in the northern extratropics. Fluctuations in the NAO
often dominate the seasonal and decadal winter climate but its
predictability on seasonal and decadal timescales is low[28,29]. If
the recent satellite data are typical of the variation in ultraviolet
fluxes in other solar cycles[14] then our results suggest shifts in the
NAO of a sizeable fraction of the interannual variability. Given
the quasiregularity of the 11-year solar cycle, our results therefore
suggest significant decadal predictability in the NAO.

Methods summary

Climate model. We use a version of the Met Office Hadley Centre general
circulation model, similar to HadGEM3 revision1.1 (ref. 15). The atmosphere
resolution is 1.875° longitude by 1.25° latitude with 85 vertical levels providing a
well-resolved middle atmosphere with an upper boundary at 85 km. The model has
an internally generated QBO. Incoming shortwave radiation is split into six bands.
The ultraviolet band, 200–320 nm, has five coefficients to describe absorption
across the band. The ocean employs a nominal 1° tripolar horizontal grid with
latitudinal grid refinement in the tropics such that the latitude spacing decreases to
1/3° on the equator and there are 42 levels in the vertical.

Ultraviolet radiation difference between solar maximum and minimum.
Measurements[9] from the SIM instrument (2004–2007) are extrapolated in time
to represent the full solar-cycle amplitude. We estimate the difference between
the solar maximum and minimum in the 200–320 nm band to be 1.2 W m^{-2}, a
4% change, and distribute this evenly across the ultraviolet band. No changes
are made in other bands.

Experiment design. An 80-year control simulation represents the solar minimum.
A 20-member ensemble of five-year simulations, with initial conditions taken
at regular intervals from the control and using the SIM-based perturbation,
represents the solar maximum. Our analysis uses the final four years of each
member, giving a total of 80 years. The figures show the difference between the
solar minimum and maximum.

Reanalysis data. ERA-40/ERA-Interim reanalysis data[30] from 1957 to 2010 are
segregated into winters with open solar magnetic flux[17,26] in the top and bottom
thirds of the values in the ERA period. The figures show the difference between the
composites of low-solar and high-solar winters. Winters following major tropical
volcanic eruptions (1963–1964, 1964–1965, 1965–1966, 1982–1983, 1983–1984,
1984–1985, 1991–1992, 1992–1993, 1993–1994) are excluded from the analysis.

Statistics. Model statistical significance is tested using a Student t-test with the
null hypothesis that the difference in means between the solar minimum and
maximum is not significantly different from zero. Reanalysis significance is assessed
using data from 1,000 pairs of randomly selected subsets of the ERA-period
years of the same size as used in the high- and low-open-solar-flux index composites.
The distribution of the differences in the means of the subsets in each pair was
used to diagnose the likelihood of the derived solar signal arising by chance.
One-tailed tests were used.

References
1. Gray, L. J. et al. Solar influences on climate. *Rev. Geophys.* **48,** RG4001 (2010).
2. Labitzke, K. Sunspots, the QBO, and the stratospheric temperature in the north polar region. *Geophys. Res. Lett.* **14,** 535–537 (1987).
3. Kodera, K. On the origin and nature of the interannual variability of the winter stratospheric circulation in the northern hemisphere. *J. Geophys. Res.* **100,** 14077–14087 (1995).
4. Kodera, K. & Kuroda, Y. Dynamical response to the solar cycle. *J. Geophys. Res.* **107,** 4749 (2002).
5. Matthes, K., Kuroda, Y., Kodera, K. & Langematz, U. Transfer of the solar signal from the stratosphere to the troposphere: Northern winter. *J. Geophys. Res.* **111,** D06108 (2006).
6. Shindell, D. T., Schmidt, G. A., Miller, R. L. & Rind, D. Northern Hemisphere winter climate response to greenhouse gas, ozone, solar, and volcanic forcing. *J. Geophys. Res.* **106,** 7193–7210 (2001).
7. Schmidt, H., Brasseur, G. P. & Giorgetta, M. A. Solar cycle signal in a general circulation and chemistry model with internally generated quasi-biennial oscillation. *J. Geophys. Res.* **115,** D00I14 (2010).
8. Tsutsui, J., Nishizawa, K. & Sassi, F. Response of the middle atmosphere to the 11-year solar cycle simulated with the whole atmosphere community climate model. *J. Geophys. Res.* **114,** D02111 (2009).
9. Harder, J. W., Fontenla, J. M., Pilewskie, P., Richard, E. C. & Woods, T. N. Trends in solar spectral irradiance variability in the visible and infrared. *Geophys. Res. Lett.* **36,** L07801 (2009).

10. Haigh, J. D. A GCM study of climate change in response to the 11-year solar cycle. *Q. J. R. Meteorol. Soc.* **125,** 871–892 (1999).
11. Haigh, J. D., Winning, A., Toumi, R. & Harder, J. W. An influence of solar spectral variations on radiative forcing of climate. *Nature* **467,** 696–699 (2010).
12. Lean, J. Evolution of the sun's spectral irradiance since the Maunder minimum. *Geophys. Res. Lett.* **27,** 2425–2428 (2000).
13. Krivova, N. A., Solanki, S. K., Wenzler, T. & Podlipnik, B. Reconstruction of solar UV irradiance since 1974. *J. Geophys. Res.* **114,** D00I04 (2009).
14. Garcia, R. R. Atmospheric physics: Solar surprise? *Nature* **467,** 668–669 (2010).
15. Hewitt, H. T. *et al.* Design and implementation of the infrastructure of HadGEM3: The next-generation Met Office climate modelling system. *Geosci. Model Dev.* **4,** 223–253 (2011).
16. Roy, I. & Haigh, J. D. Solar cycle signals in sea level pressure and sea surface temperature. *Atmos. Chem. Phys.* **10,** 3147–3153 (2010).
17. Woollings, T., Lockwood, M., Masato, G., Bell, C. & Gray, L. Enhanced signature of solar variability in Eurasian winter climate. *Geophys. Res. Lett.* **37,** L20805 (2010).
18. Hines, C. O. A possible mechanism for the production of sun–weather correlations. *J. Atmos. Sci.* **31,** 589–591 (1974).
19. Scaife, A. A. & James, I. N. Response of the stratosphere to interannual variability of tropospheric planetary waves. *Q. J. R. Meteorol. Soc.* **126,** 275–297 (2000).
20. Scaife, A. A., Knight, J. R., Vallis, G. K. & Folland, C. K. A stratospheric influence on the winter NAO and North Atlantic surface climate. *Geophys. Res. Lett.* **32,** L18715 (2005).
21. Wittman, M. A. H., Polvani, L. M., Scott, R. K. & Charlton, A. J. Stratospheric influence on baroclinic lifecycles and its connection to the Arctic Oscillation. *Geophys. Res. Lett.* **31,** L16113 (2004).
22. Simpson, I. R., Blackburn, M. & Haigh, J. D. The role of eddies in driving the tropospheric response to stratospheric heating perturbations. *J. Atmos. Sci.* **66,** 1347–1365 (2009).
23. Kodera, K., Yamazaki, K., Chiba, M. & Shibata, K. Downward propagation of upper stratospheric mean zonal wind perturbation to the troposphere. *Geophys. Res. Lett.* **17,** 1263–1266 (1990).
24. Cahalan, R. F., Wen, G., Harder, J. W. & Pilewskie, P. Temperature responses to spectral solar variability on decadal time scales. *Geophys. Res. Lett.* **37,** L07705 (2010).
25. Meehl, G. A., Arblaster, J. M., Matthes, K., Sassi, F. & van Loon, H. Amplifying the Pacific climate system response to a small 11-year solar cycle forcing. *Science* **325,** 1114–1118 (2009).
26. Lockwood, M., Harrison, R. G., Woollings, T. & Solanki, S. Are cold winters in Europe associated with low solar activity? *Environ. Res. Lett.* **5,** 024001 (2010).
27. Shindell, D. T., Schmidt, G. A., Mann, M. E., Rind, D. & Waple, A. Solar forcing of regional climate change during the Maunder minimum. *Science* **294,** 2149–2152 (2001).
28. Arribas, A. *et al.* The GloSea4 ensemble prediction system for seasonal forecasting. *Mon. Weath. Rev.* **139,** 1891–1910 (2011).
29. Kushnir, Y., Robinson, W. A., Chang, P. & Robertson, A. W. The physical basis for predicting Atlantic sector seasonal-to-interannual climate variability. *J. Clim.* **19,** 5949–5970 (2006).
30. Uppala, S. M. *et al.* The ERA-40 re-analysis. *Q. J. R. Meteorol. Soc.* **131,** 2961–3012 (2005).

Acknowledgements

Author contributions

S.I. ran the model experiments. A.A.S. and S.I. analysed the results. J.C.M. advised on adapting the radiation code. J.R.K. analysed the ERA reanalysis data and advised on statistical methods. A.A.S., S.I., J.C.M. and N.J.D. wrote the paper. All authors planned the experiment, discussed the results and commented on the manuscript.

Additional information

The authors declare no competing financial interests. Supplementary information accompanies this paper on www.nature.com/naturegeoscience. Reprints and permissions information is available online at http://www.nature.com/reprints. Correspondence and requests for materials should be addressed to S.I.